The Effect of Mean Stress on Crack Propagation in Plates Under Extension and Bending 4

by

Richard Roberts and Fazil Erdogan

December 1966

Progress Report Prepared for NASA Under Contract

NGR 39-007-011

Lehigh University

Bethlehem, Pennsylvania

The Effect of Mean Stress on Crack Propagation in Plates Under Extension and Bending*

by

Richard Roberts** and Fazil Erdogan***

ABSTRACT

A critical review of the work of Broek and Schijve for varying mean stress and a simple model representing their data are given. A comparative study of fatigue crack propagation in thin plates under fluctuating plane extension and cylindrical bending previously made by the present authors is extended to situations of nonzero mean stress. The theoretical considerations are compared to already existing data and new data obtained from 2024-T3 bare and clad aluminum specimens subjected to fully reversed and nonsymmetric bending loads.

* This study was partially supported by NASA under contract NGR 39-007-011 and NSF Grant GK-1225.

** Assistant Professor of Mechanical Engineering, Lehigh University.

*** Professor of Mechanics, Lehigh University.

1) Introduction

It has been clearly established during the last decade that the overall fatigue life of a structure may be represented by three distinct phases: crack initiation, crack propagation, and final failure.

Final failure, although extremely important since it represents the ultimate collapse of the structure, normally occurs in one or two applications of the applied loads. Thus the largest portion of a structure's fatigue life is spent in the crack initiation and crack propagation phases. This allows one to consider without any loss of generality the overall fatigue life of a structure as being composed of the crack initiation and crack propagation phases.

In very bulky structures where severe stress concentrations are not present the crack initiation phase, in general, occupies the largest portion of fatigue life. As a result of the cyclic nature of the applied loads cyclic slip occurs in the structure. This cyclic slip causes small microcracks to form. Since the type structure being considered precludes severe stress concentrations there are not any preferential locations for these microcracks to form. Thus a large number of randomly located microcracks tend to form within the same relative period of time. By the time these microcracks coalesce to form one or more macrocracks the remaining portion of fatigue life is comparatively short. In this type of structure, due to the generally complex nature of the interaction between the structure's geometry, the crack geometry, and the applied loads, the designer is forced to rely on S-N type studies and all of their ramifications.

Structures whose elements are primarily composed of thin plates and shells exhibit a different distribution of time between the crack

initiation and crack propagation phases than that found for bulky structures. In these structures macrocracks are found to be present very early in the structure's fatigue life. Although many macrocracks initially form, one dominant through crack normally emerges within a relatively short period of time. Thus it is reasonable to assume that the major portion of fatigue life for this type of structure is spent in propagating the dominant crack to some critical length at which time final failure of the structure occurs.

In thin plate and shell structures, usually the main component of loading is that which gives rise to meridional stresses. Hence, justifiably, the studies to date dealing with fatigue crack growth in thin plates have been confined to a wide plate with a central crack under repeated symmetric uniaxial loading (e.g., [1] through [10]). In spite of some ambitious attempts to account for all of the possible causes of fatigue crack propagation (e.g., [11]), the more reasonable explanations (e.g., [12]) are still partial and qualitative. The more general approaches only indicate the overwhelming complexity of the problem.

From the designers point of view, since the variables available to him are the mechanical properties of the material, the geometry, and external loads, it is quite natural to look for a continuum model to describe crack propagation. The problem of a through crack in a plate or shell structure also lends itself to simplification when compared to bulky structure. In thin plate and shell structures the problem may be idealized as being two dimensional. This simplification allows the stresses and strains in the structure to be estimated very easily in terms of continuum parameters whereas the problems encountered in bulky structures are in general intractable. The fact that in some

materials, notably in aluminum-copper alloys, crack extension occurs in every cycle [12], lends further credibility to treating crack propagation as a continuous phenomenon. Thus numerous continuum models have been proposed for crack propagation in thin sheets, each with its own experimental justification.

In some sheet-stringer structures in addition to meridional loads, the thin sheets are subjected to bending. In a recent paper, Erdogan and Roberts [13] showed that crack propagation in thin plates subjected to cylindrical bending could be predicted quanitatively using a continuum mechanics approach. The materials used in this study were 2024-T3 and 7075-T6 aluminum alloys of three thicknesses for each material. The type of bending loads employed were completely reversed thus producing a zero mean stress in the plates. The purpose of this study is to present further experimental evidence in support of their model for the 2024-T3 aluminum and extend the model to situations where the mean stress is not zero. The study also critically evaluates the work of Schijve [14] concerning the effect of mean stress on crack propagation in thin plates subjected to uniaxial tension.

2) Theoretical Considerations

In a recent paper [13] the model of crack propagation proposed by Schijve [12] was used as a basis for making a rational comparison between crack propagation caused by extensional loads and crack propagation caused by bending loads. Without going into the details, Schijve's model, which assumed that crack extension is a geometric consequence of dislocation movements, may be written as

$$\frac{\Delta a}{\Delta n} = \varphi mb \tag{1}$$

where a is the half crack length, n is the number of cycles, m is the total number of moving dislocations which could possibly contribute to crack extension, b is the magnitude of the Burgers vector, and the coefficient φ represents the fraction of the total number of dislocations effectively contributing to the crack extension ($0 < \varphi < 1$).

At this point, in order to relate the quantities φ and m to some continuum parameter, it was argued [13] that m would be primarily composed of the dislocations concentrated in the plastic zone at the crack tip and that this could be related to a characteristic length of the plastic zone, P. Although it was not used at the time, it was further argued for situations where a non-zero mean stress occurred that the quantity m would be best described in terms of the maximum value of the representive length P or P max. Thus m may be functionally expressed as:

$$m = f_1(P_{max}) \tag{2}$$

In relating the quantity φ to a continuum parameter it was reasoned that φ would be proportional to the cyclic range of the plastic strains in the plastic zone since stress has very little meaning in this region and that the plastic strains would be a better measure of the severity of the forces compelling the dislocations to move. Again the plastic strains at the crack tip may be related to the characteristic length P and the strain range to ΔP. Therefore φ may be assumed to be a function of ΔP:

$$\varphi = f_1(\Delta P) \tag{3}$$

The only thing that may be said about the functions f_1 and f_2 is that they should be smooth monotonically increasing functions and vanish for $P_{max} = 0$ and $\Delta P = 0$ respectively. Therefore within a given range of P max and ΔP one may approximate the functions f_1 and f_2 as

$$f_1(P_{max}) = A_1(P_{max})^{\alpha_1} \quad ; \quad f_2(\Delta P) = A_2(\Delta P)^{\alpha_2} \tag{4}$$

where A_1, A_2, α_1 and α_2 are positive constants. Combining the constants and, over the appropriate ranges of P_{max} and ΔP, considering the growth as a continuous process, (1) may be written as

$$\frac{da}{dn} = A(P_{max})^{\alpha_1}(\Delta P)^{\alpha_2} \tag{5}$$

As pointed out in the original work [13] equation (5) is not an attempt to produce an all encompassing law of crack growth or to even add another "power law" of crack propagation to those already existing. In general the functions f_1 and f_2 will vary from material to material. It is further expected that even for the same material A_1, A_2, α_1 and α_2 will vary depending upon the operating ranges of P_{max} and ΔP.

If the representative length, P, is taken as the dimension of the plastic zone along the prolongation of the crack, it may be estimated in various ways. The estimate given by Dugdale [15] appears to be fairly realistic and seems to agree with the available data. The estimate is based on the removal of the stress singularity at the crack tip by introducing a rigid plastic strip and, for a wide plate under plane stress, is found to be

$$P = \sec\left[\frac{\pi\sigma}{2\sigma_y} - 1\right] a \tag{6}$$

where a is the half crack length, σ the applied stress, and σ_y the

yield stress. Dugdale's technique has been used by Rosenfield, Dai, and Hahn [16] to solve more complex problems with great success. Roberts [17] has also used this type of analysis for determining the plastic zone size for a thin plate subjected to cylindrical bending leading to

$$P = \sec\left[\frac{\pi \sigma_b}{4\sigma_y} - 1\right] a \tag{7}$$

where σ_b is the surface stress in the plate a great distance from the crack. Equations (6) and (7) may be approximated for small values of the ratios (σ/σ_y) and (σ_b/σ_y) as

$$P = \frac{1}{2}\left(\frac{\pi\sigma}{2\sigma_y}\right)^2 a = \frac{1}{2}\left(\frac{\pi}{2\sigma_y}\right)^2 K^2 \tag{6A}$$

and

$$P = \frac{1}{2}\left(\frac{\sigma_b}{4\sigma_y}\right)^2 a = \frac{1}{2}\left(\frac{\pi}{4\sigma_y}\right)^2 K_b^2 \tag{7A}$$

where $K = \sigma\sqrt{a}$ is the stress intensity factor for tension and $K_b = \sigma_b \sqrt{a}$ the stress intensity factor for bending. Equations (6A) and (7A) predict for small values of the ratio of the remotely applied stress to the yield stress that the plastic zones for tension and bending are both proportional to the square of the stress intensity factor.

Rice [18] in a fairly exhaustive survey article of his work and the work of others showed that for small scale yielding the plastic zone could be quite realistically represented by the stress intensity factor for (σ/σ_y) less than 0.4. He further found that the change in the plastic zone size due to the cyclic nature of the load could be related to the range value of the stress intensity factor, ΔK, for values of σ/σ_y less than 0.8, where ΔK is defined as $(K_{max} - K_{min})/2$. Rice argued that, since a cyclic load may be characterized by its maximum

and range values, the planar geometry of the cracked body and the external loads are sensed at the crack tip for small scale yielding only through K_{max} and ΔK. This led him to propose a functional form for a model of crack propagation as

$$\frac{da}{dn} = f_3(\Delta K, K_{max}) \tag{8}$$

In view of Rice's findings one may write equations (4) as

$$\begin{aligned} f_1(P_{max}) &= A_3(K_{max})^{\alpha_3} \qquad \frac{\sigma}{\sigma_y} < 0.4 \\ f_2(\Delta P) &= A_4(\Delta K)^{\alpha_4} \qquad \frac{\sigma}{\sigma_y} < 0.8 \end{aligned} \tag{9}$$

if P and ΔP are assumed to be proportional to some power of K_{max} and ΔK respectively. Using equations (9) and (5) one obtains

$$\frac{da}{dn} = A_5(K_{max})^{\alpha_3}(\Delta K)^{\alpha_4} \qquad \frac{\sigma}{\sigma_y} < 0.4 \tag{10}$$

$$\frac{da}{dn} = A_6(P_{max})^{\alpha_3}(\Delta K)^{\alpha_4} \qquad \frac{\sigma}{\sigma_y} < 0.8 \tag{11}$$

If K_{max} is replaced by $K_m + K_a$ where K_m equals $(K_{max} + K_{min})/2$ and β defined as $\beta = K_m/K_a$ equation (10) can be written as

$$\frac{da}{dn} = A_5(1 + \beta)^{\alpha_3}(\Delta K)^{\alpha_3+\alpha_4} \tag{12}$$

To examine the difference between crack propagation in tension and bending equations (6A) and (7A) may be substituted into equation (5) giving

$$\frac{da}{dn} = A_6 2^{-(\alpha_1+\alpha_2)} \left(\frac{\pi}{2\sigma_y}\right)^{2(\alpha_1+\alpha_2)} (1+\beta)^{2\alpha_1} (\Delta K)^{2(\alpha_1+\alpha_2)}$$

(in tension) (13)

$$\frac{da}{dn} = A_7 2^{-(\alpha_{1b}+\alpha_{2b})} \left(\frac{\pi}{4\sigma_y}\right)^{2(\alpha_{1b}+\alpha_{2b})} (1+\beta)^{2\alpha_{1b}} (\Delta K)^{2(\alpha_{1b}+\alpha_{2b})}$$

(in bending) (14)

Because of the similarity of fracture modes if we assume that $A_6 = A_7$, $\alpha_1 = \alpha_{1b}$ and $\alpha_2 = \alpha_{2b}$, by combining the constants (13) and (14) may be written as

$$\frac{da}{dn} = B(1+\beta)^{2\alpha_1} (\Delta K)^{2(\alpha_1+\alpha_2)} \quad \text{(in tension)} \qquad (15)$$

$$\frac{da}{dn} = B(1+\beta)^{2\alpha_1} (\Delta K/2)^{2(\alpha_1+\alpha_2)} \quad \text{(in bending)} \qquad (16)$$

where the limitation $\sigma/\sigma_y < 0.4$ is implied in equations (12) through (16).

3) Experimental Results

The test specimens consisted of 2024-T3 bare and clad commercial aluminum alloys. Triangular specimens cut from 12" x 18" plates were used. In the plane of the crack the plate width was 8.625". The length of the artificial cut (consisting of 0.04" diameter hole, 0.015" wide saw cut and a tap with a razor blade) was approximately 0.2 ". Before putting the cut in, strain gages placed at various locations indicated that in the central trapezoidal portion of the cantilever plates the strains were constant within 3%. The testing machine was a constant

displacement type running at 140 CPM. The machine was adjustable so that either a fully reversed displacement (e.g., zero mean stress) or a non-symmetric displacement (e.g., non zero mean stress) could be obtained. Static deflection tests with dead weights performed at various crack lengths showed that the stiffness of the plate and the strains away from the crack remained constant within a few percent up to plate width-to-crack length ratio, $(b/a) = 5$. For larger crack lengths the bulging around the crack became significant enough to cause a reduction in the stiffness. Thus all tests were stopped at about 1.8 in. crack lengths.

The measurement of the tip-to-tip crack length was started after a natural fatigue crack was formed and extended approximately 0.01 in. at each tip which roughly corresponds to the depth of the triangular notch put by the razor blade. The crack length was measured by a fifty power traveling microscope by stopping the test on the peak of the tension cycle. The sensitivity of the microscope ($\pm 10^{-5}$ in) is found to be higher than the accuracy within which the "crack tip" could be defined. The indefiniteness of the detection of the crack tip was partly due to the surface roughening in clad specimens. In the bare specimens there was no surface roughening, however some contraction in thickness at the crack tips was observable.

The results of the present bending tests for $\beta = 0$ and various stress amplitudes are shown in Figure 1. The results for $\beta = 1$ are shown in Figure 2, β being defined for the side of the plate having the largest tensile stress during the cycle. In the present study the tests at $\beta = 1$ were conducted by giving the tests specimens a one sided deflection (e.g., zero to a maximum deflection). The comparable results for plane extensional loading and $\beta = 0$ are shown in Figure 3 [7].

Figures 4, 5 and 6 show some of the results for the individual plate thicknesses. The scatter bands covering 95 percent of the total population for a least square straight line fit and for $2(\alpha_1 + \alpha_2) = 4$ are also shown in the Figures 4 through 6.

The values obtained for B, and $2(\alpha_1 + \alpha_2)$ for $\beta = 0$ and $\beta = 1$ are given in tabular form in Table I. For the sake of completeness the original values given in reference [13] are also included. It should be pointed out that the B values for $\beta = 0$ in reference [13] were for d(2a)/dn but were reported as being for da/dn. These values have been corrected and are now correct for da/dn. Table II and III gives the values of B, α_1, and α_2 obtained from Broek and Schijve's data [14] for various values of β.

4) Discussion

Before discussing the results of the bending tests for $\beta = 0$ and $\beta = 1$ a detailed examination will be made of the results given by Broek and Schijve for plane extension [14].

Broek and Schijve in their study of mean stress ran very carefully controlled tests where they varied the values of mean stress and stress amplitude in thin (0.08 in) plates subjected to uniaxial tension. The materials studied were 2024-T3 and 7075-T6 bare aluminum alloys. The values of σ_m and σ_a, the mean and amplitude stresses respectively are given in Table II and III. σ_m is defined as $(\sigma_{max} + \sigma_{min})/2$ and σ_a as $(\sigma_{max} - \sigma_{min})/2$. Since the maximum stress in all of Broek and Schijve's tests on the 2024-T3 and 7075-T6 aluminum alloys never exceded one half of the yield stress, one would expect that the stress intensity factor should be the simplest single variable for representing the

external loading and the geometry. With this in mind an equation of the form

$$\frac{da}{dn} = B(1 + \beta)^{2\alpha_1}(\Delta K)^{2(\alpha_1+\alpha_2)}$$

was fitted to the data in reference [14]. To account for the finite size of the test specimens the very precise correction factor for the stress intensity factor given by Isida [19] was used.

In performing the statistical fit to Broek and Schijve's data the value of β was fixed and ΔK was the independent variable. Thus values of $2(\alpha_1 + \alpha_2)$ and $B(1 + \beta)^{\alpha_1}$ were obtained. From Tables II and III it is seen that the value of $2(\alpha_1 + \alpha_2)$ is not in general a constant for different values of β. Table II and III, along with the values of B, α_1 and α_2, gives the value of r, the correlation coefficient. The fact that this value is so close to unity implies that the assumption of the crack growth rate being proportional to some power of ΔK is well justified. For the 2024-T3 material the values of $2(\alpha_1 + \alpha_2)$ ranged between 4.15 and 3.05 with an average value of 3.62. For the 7075-T6 material the values of $2(\alpha_1 + \alpha_2)$ ranged between 4.34 and 3.4 with an average value of 3.90. It should be pointed out that the values of $2(\alpha_1 + \alpha_2)$, the slope of the da/dn versus K line on a log-log plot, is independent of the choice K_{max} or ΔK for the independent variable since K_{max} and ΔK are related as follows:

$$\Delta K = (K_{max} - K_{min})/2$$

and defining γ as

$$\gamma = \frac{K_{min}}{K_{max}}$$

equation (12) can be written as

$$\frac{da}{dn} = A_5(1 + \beta)^{\alpha_3}\left(\frac{1 - \gamma}{2}\right)^{\alpha_4}(K_{max})^{\alpha_3+\alpha_4} \tag{17}$$

Thus the same slope will be obtained independently of the choice of K_{max} or ΔK since β and γ are constants for tests run by Broek and Schijve.

At the end of their paper Broek and Schijve recommend an equation of the form

$$\frac{da}{dn} = C_1 e^{-C_2 R}(K_{max})^3\left(1 + 10\frac{a^2}{\omega^2}\right)$$

where C_1 and C_2 are constants, ω the half plate width and $R = \sigma_{min}/\sigma_{max}$. This equation was deduced by visually calling the slope of the da/dn versus K_{max} plates as being equal to three and using this to obtain the remaining functional form of the equation. It has just been shown that the slope will be independent of the choice between K_{max} and ΔK and that the slope for ΔK was not, in general, equal to three. Thus it is believed that the equation to be derived now will not only be a simpler one to use but a better approximation of crack growth rates over the range of data given by Broek and Schijve.

At this point, based on the values of $2(\alpha_1 + \alpha_2)$ it is obvious that there is no simple power function which will describe the crack growth rate for different values of β. However, if the average value of $2(\alpha_1 + \alpha_2)$ is used to approximate the slope of all of the data, some valuable information can be obtained about the influence of β on the crack growth rate. Fixing the value of $2(\alpha_1 + \alpha_2)$ for the 2024-T3 at 3.62 and the value of $2(\alpha_1 + \alpha_2)$ for the 7075-T6 at 3.90 values of $B(1 + \beta)^{2\alpha_1}$ were obtained. These values are given in Tables II and III.

Values for $B(1 + \beta)^{2\alpha_1}$ were also obtained for $2(\alpha_1 + \alpha_2) = 4$ as a means of comparison with already existing data.

Now by taking the values of $B(1 + \beta)^{2\alpha_1}$ and plotting them as a log-log plot it was found that all of the points fell on a relatively straight line (Fig. 7 and 8). By statistically fitting a straight line to the points values of B and $2\alpha_1$ were obtained. These are given in Tables II and III. The correlation coefficient for these lines although not given were also very near unity.

Thus, for fluctuating tension, the following equations are put forward as best representing Broek and Schijve's data over the whole range of β.

$$\frac{da}{dn} = 2.68 \times 10^{-19}(1 + \beta)^{1.72}(\Delta K)^{3.62} \qquad (2024\text{-}T3) \quad (19)$$

$$\frac{da}{dn} = 6.22 \times 10^{-20}(1 + \beta)^{1.78}(\Delta K)^{3.90} \qquad (7075\text{-}T6) \quad (20)$$

As a means of checking this type of functional form with another source of data the results of reference [7] were used. Since this data was evaluated at $2(\alpha_1 + \alpha_2) = 4$ and $\beta = 0$, the values of B for $2(\alpha_1 + \alpha_2) = 4$ from Tables II and III should compare with the values in Tables I. For the 2024-T3 material the B value obtained from Broek and Schijve's data is 8.7×10^{-21} while the data from reference [7] gives 6.0×10^{-21}. This is closer than one would normally hope for in this type of work. For the 7075-T6, Broek and Schijve's data gives $B = 2.95 \times 10^{-20}$ while the data from reference 7 gives $B = 6.5 \times 10^{-21}$. This apparent discrepancy here is predictable. For the 2024-T3 aluminum the material properties were almost identical in both studies while for the 7075-T6

material, although the yields were similar in value, the material used by Broek and Schijve was less ductile by about 30 percent. Thus it is expected that Broek and Schijve's material would exhibit a high rate of crack growth at similar ΔK and β levels.

In the paper by Erdogan and Roberts [13] it was also observed that there was no single value of $2(\alpha_1 + \alpha_2)$ which would represent all of the data obtained for cylindrical bending. In order to make a comparison of crack propagation rates due to extension and bending they used a value of $2(\alpha_1 + \alpha_2) = 4$. Since a great deal of data has already been obtained for plane extension it would be a great help to be able to predict crack growth rates due to bending loads from the existing extensional data. Thus an experimentally determined quanity λ was defined so that when $\beta = 0$

$$\left(\frac{da}{dn}\right)_t = (B)_t \, \Delta K^4 \quad ; \quad \left(\frac{da}{dn}\right)_b = (B)_b (\Delta K_b)^4 = (B_t)(\lambda \, \Delta K_b)^4 \qquad (21)$$

where the subscript t and b referes to tension and bending respectively. Writing equations (15) and (16) for $\beta = 0$ as

$$\left(\frac{da}{dn}\right)_t = B \, \Delta K^{2(\alpha_1+\alpha_2)} \quad ; \quad \left(\frac{da}{dn}\right)_b = B(0.5 \, \Delta K)^{2(\alpha_1+\alpha_2)} \qquad (22)$$

it is seen that the theoretical value of λ which appears in (21) is 0.5. The experimental values of λ from the present study for two thicknesses of the 2024-T3 alloy appear in Table I along with the original values found in [13].

The agreement seems to be fairly good implying that, in the absence of experimental data, for a quick estimate of crack growth rate in plates under cylindrical bending for $\beta = 0$ one may use the extension data for $\beta = 0$ by merely replacing K by $K_b/2$. Selecting a

value for $2(\alpha_1 + \alpha_2)$ other than 4, the present data indicates that, for the same stress intensity factor in extension and bending of thin plates, the relation

$$\left(\frac{da}{dn}\right)_{\text{bending}} = 2^{-2(\alpha_1+\alpha_2)} \left(\frac{da}{dn}\right)_{\text{extension}} \tag{23}$$

is approximately valid and may be used to estimate the crack growth rate in bending. Thus the results of reference [13] and the present results for $\beta = 0$ indicate that over a wide range of plate thicknesses (e.g., 0.05 in. to 0.16 in.) for the 2024-T3 alloy equation (23) may be used to estimate crack growth rates.

Concerning the value of λ defined in (21) it should be pointed out that the theoretical value of λ being 0.5 is based on, among other simplifications, the fact that the plate is "thin", the elastic stress distribution is linear in δ, the distance from the mid-plane, and a plastic hinge develops ahead of the crack tip. However, as the plate thickness increases, none of these assumptions will be valid, the nonlinearity of the stress distribution in δ will become more significant and in limit the stress state will approach that of plane strain. Hence, it would be expected that the value of λ will increase with the increasing plate thickness.* On the other hand for relatively thin plates, this variation in λ is somewhat compensated by the fact that as a result of the plastic hinge never fully developing the theoretical value of λ for "thin" plates would be actually less than 0.5.

In order to study the effect of non zero values of β for cylindrical bending, two 0.05 inch thick 2024-T3 alclad specimens were run at $\beta = 1$.

* In plane strain the plastic zone size is approximately one half of that for plane stress; thus for this case the value of λ would be approximately $1/\sqrt{2}$.

The values of $B(1 + \beta)^{2\alpha_1}$, $2(\alpha_1 + \alpha_2)$ and $B(1 + \beta)^{2\alpha_1}$ for $2(\alpha_1 + \alpha_2) = 4$ are given in Table I. Since it is still convenient to be able to estimate crack growth rates due to bending loads which produce nonzero values of β from already existing tensile data, a comparison will be made based on the common slope $2(\alpha_1 + \alpha_2) = 4$. Taking the values of B and $2\alpha_1$ found in Table II an equation of the form

$$\frac{da}{dn} = 8.7 \times 10^{-21}(1 + \beta)^{1.99}(\Delta K)^4 \tag{24}$$

can be written for the 2024-T3 material. If the theoretical value of $\lambda = (0.5)$ is applied to ΔK and β is set equal to 1, equation (24) becomes

$$\frac{da}{dn} = 2.16 \times 10^{-21}(\Delta K_b)^4 \tag{25}$$

As seen from Table I the value of $B(1 + \beta)^{2\alpha_1}$ for $\beta = 1$ and $2(\alpha_1 + \alpha_2)$ is 3.02×10^{-21}. Thus there is satisfactory agreement between the proposed model and the experimental values. However, since only one non zero value of β was used, this result must be viewed with caution.

It should be noted although some of the bending data does not meet the limitation of $\sigma/\sigma_y < 0.4$ that the values of the correlation coefficients, r, indicate that the functional form of the model is still acceptable as a means of correlating crack growth data.

5) Conclusions

i. In any study of crack propagation where a model of crack propagation is being evaluated by fitting a straight line to the data, linear regression theory should be prefered over the reliance on a straight edge-human eye combination if one desires to accurately know the slope of the best fit line.

ii. For the data given by Broek and Schijve an expression of the form

$$\frac{da}{dn} = B(1 + \beta)^{2\alpha_1}(\Delta K)^{2(\alpha_1+\alpha_2)}$$

may be used very satisfactorily if $2(\alpha_1 + \alpha_2)$ is taken as the average value of the $2(\alpha_1 + \alpha_2)$ values. This form is easier to use than the one proposed by Broek and Schijve since ΔK and β are the most representative parameters in describing the effect of the applied load and planar geometry on the stress field near the crack tip for small scale yielding.

iii. For cylindrical bending a quick estimate of crack propagation rates may be made where other data is lacking by using data for plane extension. This is done by modifying ΔK in the above equation by a factor $\lambda = 0.5$ or

$$\frac{da}{dn} = B(1 + \beta)^{2\alpha_1}(0.5\,\Delta K)^{2(\alpha_1+\alpha_2)}$$

where B, $2\alpha_1$ and $2(\alpha_1 + \alpha_2)$ are obtained from the plane extension data.

6) Acknowledgement

The authors are indebted to Mr. John J. Kibler who obtained the 2024-T3 bending data for t = 0.16 in., 0.05 in., $\beta = 0$, and t = 0.05 in., $\beta = 1$.

References

1. A.K. Head, "The growth of fatigue cracks", Phil. Mag., vol. 44, 1953, pp. 925-938.

2. N.E. Frost and D.S. Dugdale, "The Propagation of fatigue cracks in sheet specimens", Jour. Mech. Phy. Solids, 1958, p. 92.

3. H.W. Liu, "Crack propagation in thin metal sheets under repeated loading", The Journal of Basic Engineering, Trans. ASME, Series D, 1961, p. 23.

4. P.C. Paris, "Crack propagation caused by fluctuating loads", ASME Paper No. 62-Met-3.

5. P.C. Paris, F. Erdogan, "A critical analysis of crack propagation laws", The Journal of Basic Engineering, Trans. ASME, Series D, 1963, p. 528.

6. D.R. Donaldson, W.E. Anderson, "Crack propagation behavior of some airframe materials", Proceedings of the Crack Propagation Symposium, Cranfield, England, 1961.

7. W. Illg, A.J. McEvily, "The rate of fatigue crack propagation for two aluminum alloys under completely reversed loading", NASA TND-52, Oct. 1959.

8. S.R. Valuri, "A unified engineering theory of high stress level fatigue", Aerospace Engineering, vol. 20, Oct. 1961, p. 18.

9. J. Schijve, "Fatigue crack propagation in light alloy sheet material", Advances in Aeronautical Sciences, vol. 3, p. 387, Pergamon Press, 1960.

10. C.T. Yang, "A study of the law of crack propagation", ASME, Paper No. 64 - WA/Met.-6.

11. S.R. Valuri, J.B. Glassco, G.E. Bockrath, "Further considerations concerning a theory of crack propagation in metal fatigue", Engineering Paper No. 1695, GALCIT SM 63-16, July 1963.

12. J. Schijve, "Analysis of the fatigue phenomenon in aluminum alloys", N.L.R. TR M. 2122, April 1964.

13. F. Erdogan, R. Roberts, "A Comparative Study of Crack Propagation in Plates Under Extension and Bending", Presented at the International Conference on Fracture, Sendai, Japan, Sept. 1965.

14. D. Broek, J. Schijve, "The influence of the mean stress on the propagation of fatigue crack in aluminum alloy sheet", N.L.R. (National Aero- and Astronautical Research Institute, Amsterdam) Report M. 2111, 1963.

15. D.S. Dugdale, "Yielding of steel sheets containing slits", Jour. Mech. Phys. Solids, vol. 8, p. 100, 1960.

16. A.R. Rosenfield, P.K. Dai, and G.T. Hahn, "Crack Extension and Propagation Under Plane Stress", Presented at the International Conference on Fracture, Sendai, Japan, Sept. 1965.

17. R. Roberts, "On the Rate of Crack Propagation Due to Fluctuating Bending Loads", a Ph.D. thesis, Lehigh University, Bethlehem, Pa., 1964.

18. J.R. Rice, "The Mechanics of Crack Tip Deformation and Extension by Fatigue", Presented at the annual ASTM meeting, Atlantic City, N.J., 1966.

19. M. Isida, "The Effect of Longitudinal Stiffeners in a Cracked Plate Under Tension", Proceedings, Fourth U.S. Congress of Applied Mechanics, 1962.

TABLE I

	No. of Plates	Thickness in.	Range of σ_{max}/σ_y	B	$2(\alpha_1+\alpha_2)$	r	$B \times 10^{22}$	λ $2(\alpha_1+\alpha_2)=4$
7075-T6 Bare & Clad Bending; $\beta=0$ * Ref. 13	3	0.050*	0.346—0.475	2.62×10^{-18}	3.06	0.87	2.90	0.460
	8	0.100*	0.446—0.826	8.80×10^{-19}	3.21	0.96	3.25	0.474
	4	0.120*	0.495—0.672	3.80×10^{-17}	2.83	0.99	3.35	0.479
2024-T3 Bare & Clad Bending; $\beta=0$ * Ref. 13	4	0.050	0.277—0.418	5.35×10^{-23}	4.19	0.96	3.27	0.483
	7	0.080*	0.232—0.668	5.20×10^{-24}	4.43	0.97	3.55	0.493
	8	0.100*	0.289—0.785	1.08×10^{-23}	4.35	0.97	3.80	0.500
	6	0.125*	0.358—0.693	3.99×10^{-22}	3.99	0.99	3.85	0.502
	6	0.160	0.439—0.656	9.20×10^{-18}	2.89	0.98	2.27	0.441
2024-T3 Clad Bending; $\beta=1$	2	0.050	0.308	1.19×10^{-23}	4.63	0.98	30.2	
7075-T6 Ref. 7 Extension $\beta=0$	3	0.081	0.081—0.402	4.12×10^{-20}	3.68	0.98	65.0	
2024-T3 Ref. 7 Extension $\beta=0$	5	0.081	0.113—0.565	2.09×10^{-20}	3.84	0.99	60.0	

TABLE II

2024-T3, Ref. 14

β	$2(\alpha_1+\alpha_2)$	r	$2(\alpha_1+\alpha_2) = 3.62$			$2(\alpha_1+\alpha_2) = 4.0$		
			$B(1+\beta)^{2\alpha_1} \times 10^{18}$	$2\alpha_1$	$B \times 10^{19}$	$B(1+\beta)^{2\alpha_1} \times 10^{20}$	$2\alpha_1$	$B \times 10^{21}$
4.80	3.584	0.988	3.715	1.72	2.679	18.941	1.99	8.700
3.00	3.639	0.982	2.332			10.125		
1.85	4.176	0.982	1.544			5.673		
3.60	3.814	0.967	2.827			13.887		
2.25	3.697	0.980	1.661			7.083		
1.38	3.816	0.984	0.961			3.470		
1.80	3.378	0.981	1.428			6.740		
1.41	3.445	0.979	1.112			4.877		
1.13	3.048	0.976	0.719			2.957		

TABLE III

7075-T6, Ref. 14

β	$2(\alpha_1+\alpha_2)$	γ	$2(\alpha_1+\alpha_2) = 3.9$			$2(\alpha_1+\alpha_2) = 4.0$		
			$B(1+\beta)^{2\alpha_1} \times 10^{19}$	$2\alpha_1$	$B \times 10^{20}$	$B(1+\beta)^{2\alpha_1} \times 10^{19}$	$2\alpha_1$	$B \times 10^{20}$
4.80	4.199	0.989	28.719	1.78	6.221	13.122	1.64	2.945
3.00	4.262	0.983	14.371			6.297		
1.85	4.343	0.983	5.148			2.203		
3.60	3.817	0.989	18.559			8.439		
2.25	3.731	0.977	9.594			4.222		
1.38	4.208	0.991	4.272			1.814		
1.80	3.462	0.984	7.390			3.344		
1.41	3.463	0.984	4.704			2.077		
1.13	3.644	0.976	2.939			1.275		

FIGURE 1.

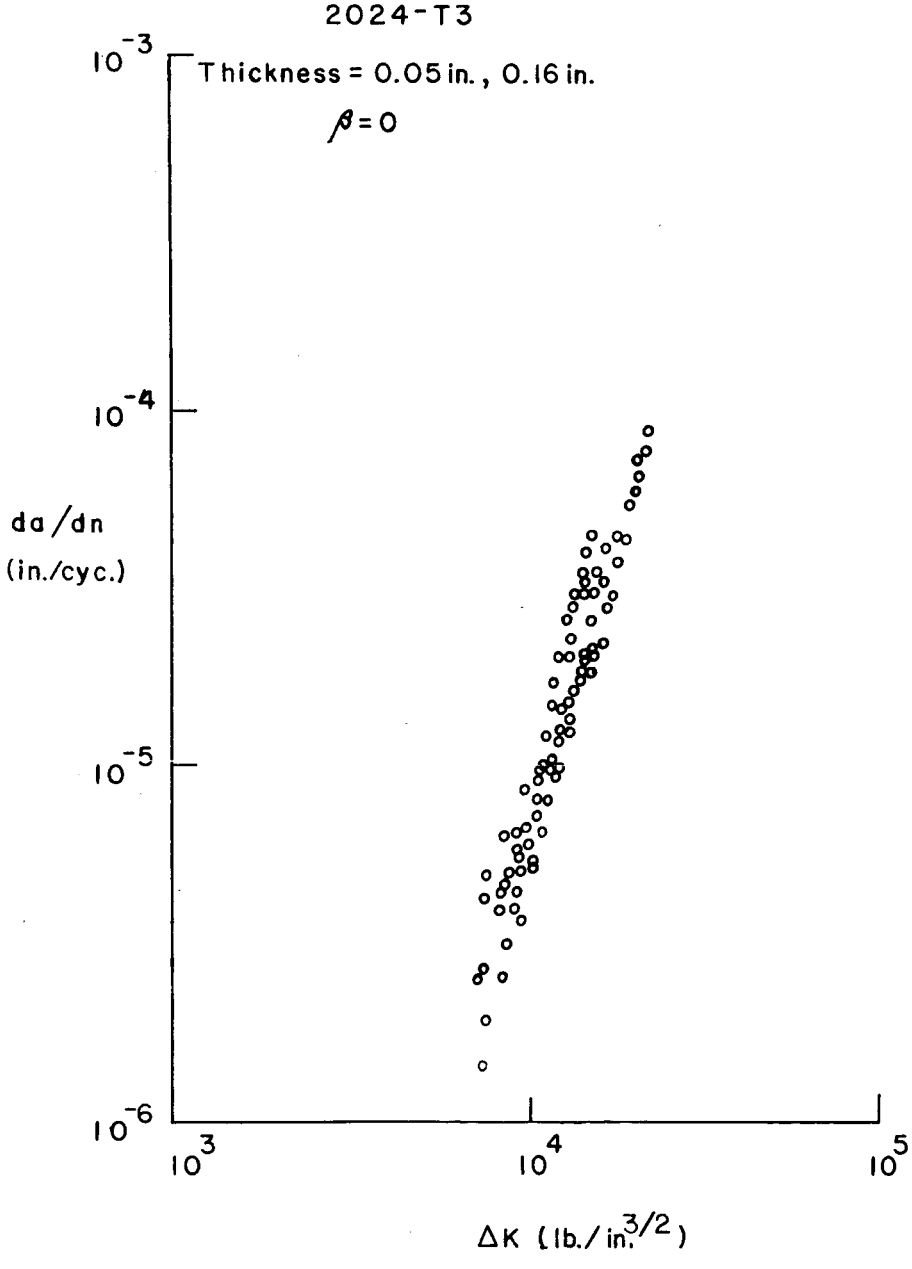
2024-T3
Thickness = 0.05 in., 0.16 in.
β = 0
10^-3
10^-4
10^-5
10^-6
da/dn
(in./cyc.)
10^3
10^4
10^5
ΔK (lb./in.^3/2)

FIGURE 2.

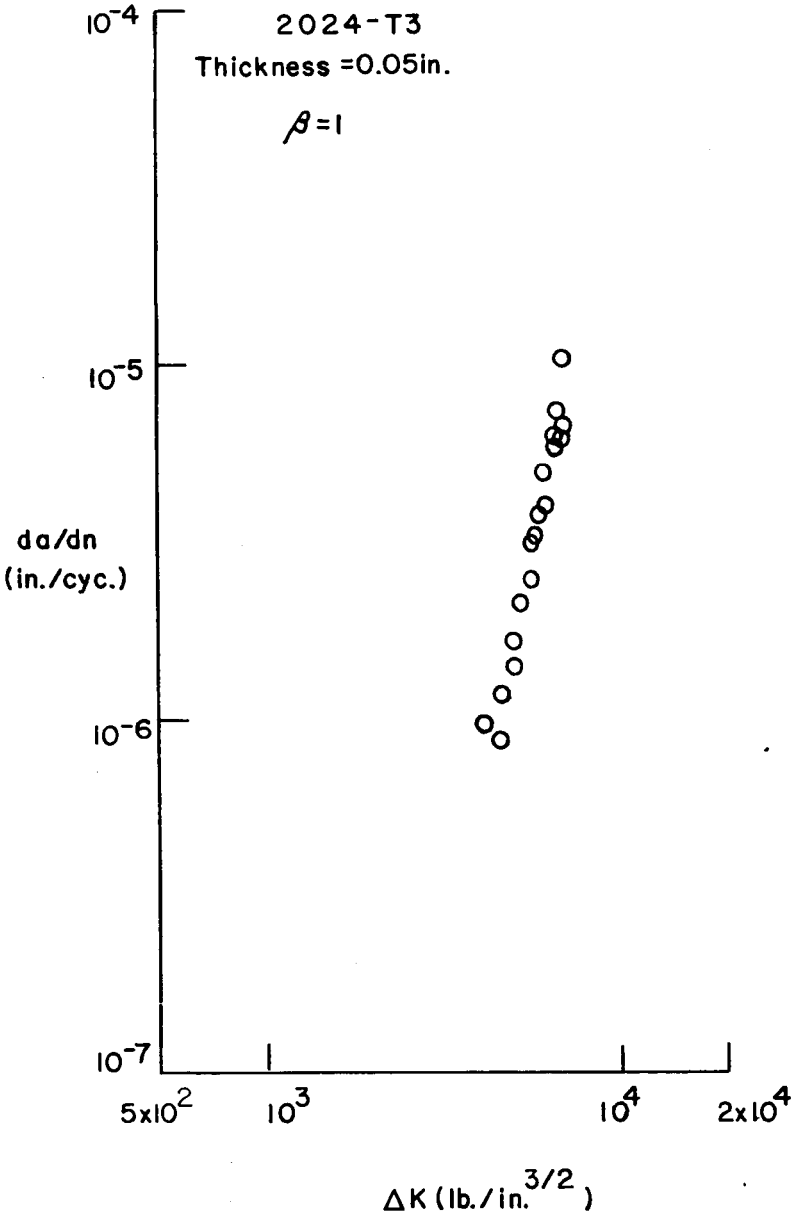
2024-T3
Thickness =0.05in.
β=1
10^-4
10^-5
10^-6
10^-7
da/dn
(in./cyc.)
5x10^2
10^3
10^4
2x10^4
ΔK (lb./in.^3/2)

FIGURE 3.

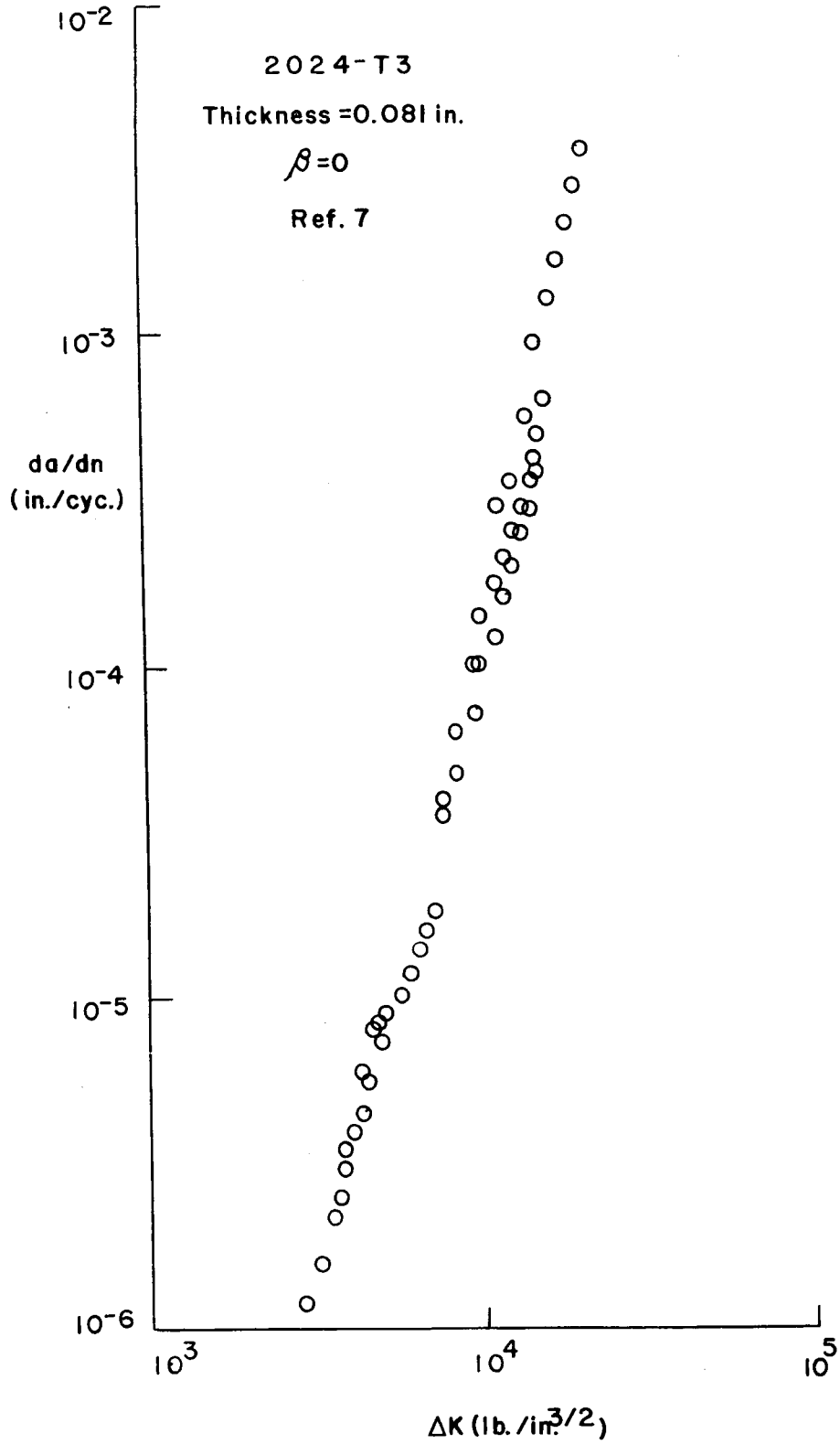
2024-T3
Thickness =0.081 in.
β=0
Ref. 7
10^-2
10^-3
10^-4
10^-5
10^-6
da/dn
(in./cyc.)
10^3
10^4
10^5
ΔK (lb./in.^3/2)

FIGURE 4.

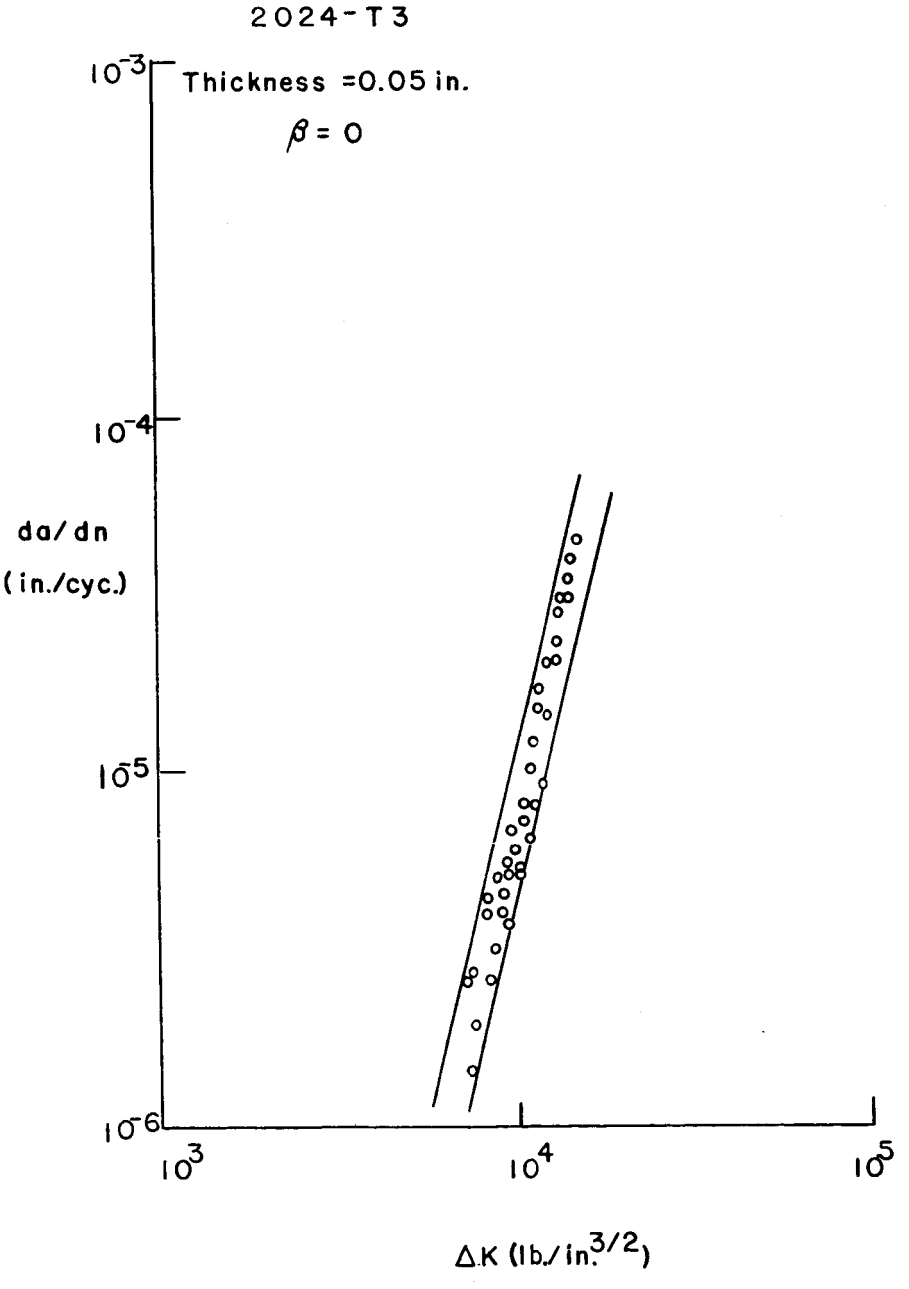
2024-T3
Thickness =0.05 in.
β = 0
10^-3
10^-4
10^-5
10^-6
da/dn
(in./cyc.)
10^3
10^4
10^5
ΔK (lb./in.^3/2)

FIGURE 5.

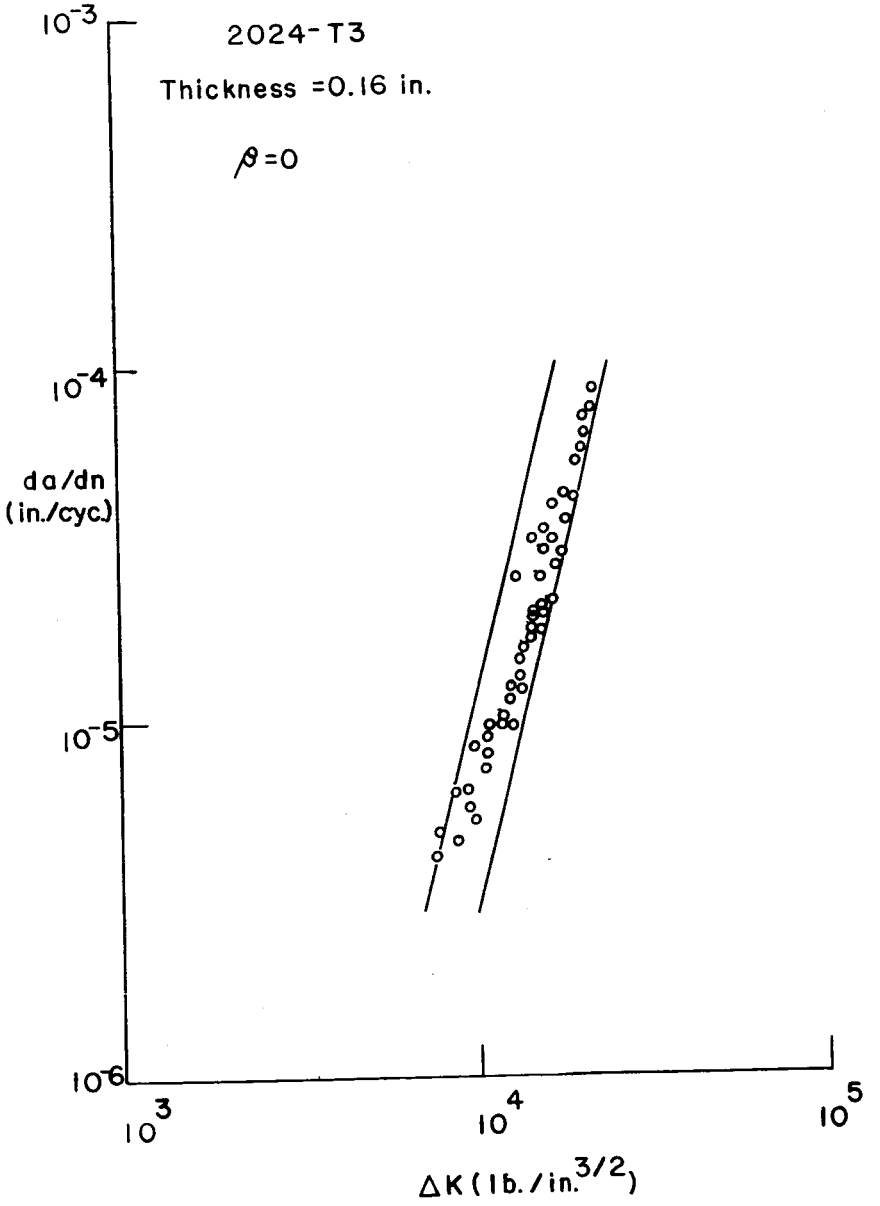
2024-T3
Thickness =0.16 in.
β=0
10^-3
10^-4
10^-5
10^-6
da/dn
(in./cyc.)
10^3
10^4
10^5
ΔK (lb./in.^3/2)

FIGURE 6.

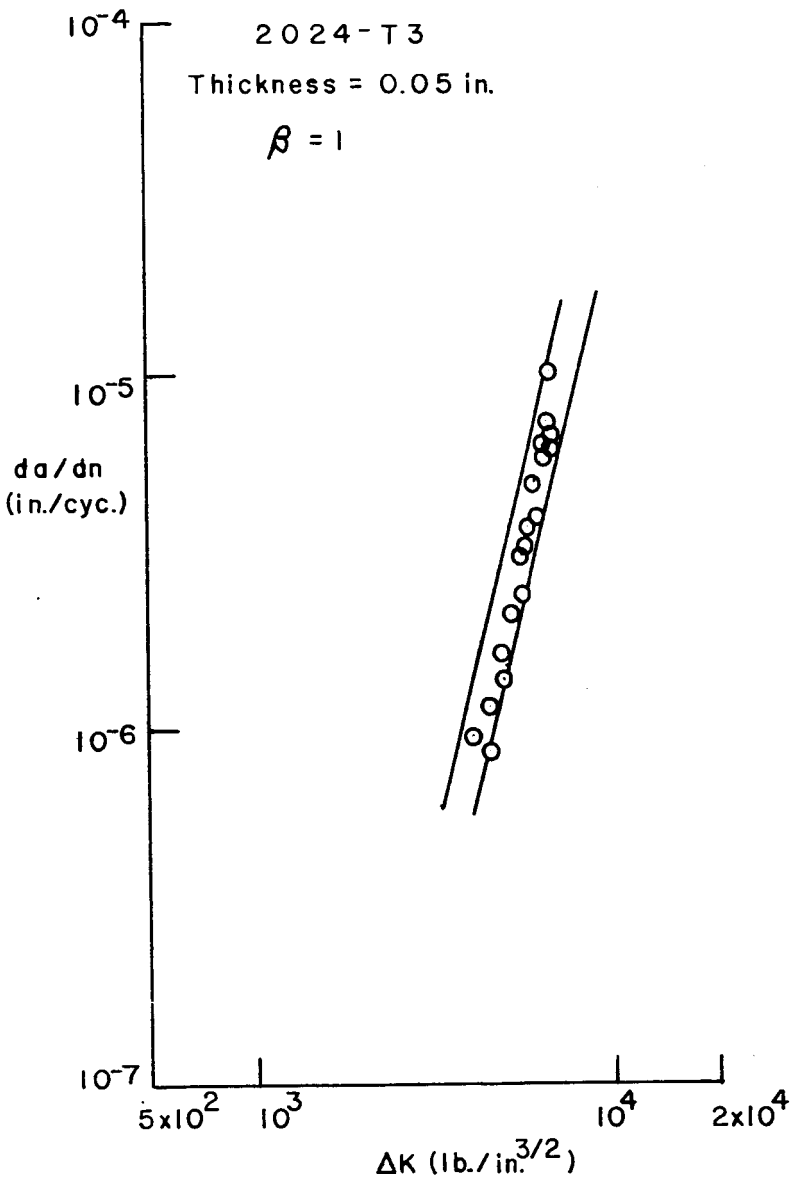
2024-T3
Thickness = 0.05 in.
β = 1
10^-4
10^-5
10^-6
10^-7
da/dn
(in./cyc.)
5x10^2
10^3
10^4
2x10^4
ΔK (lb./in.^3/2)

FIGURE 7.

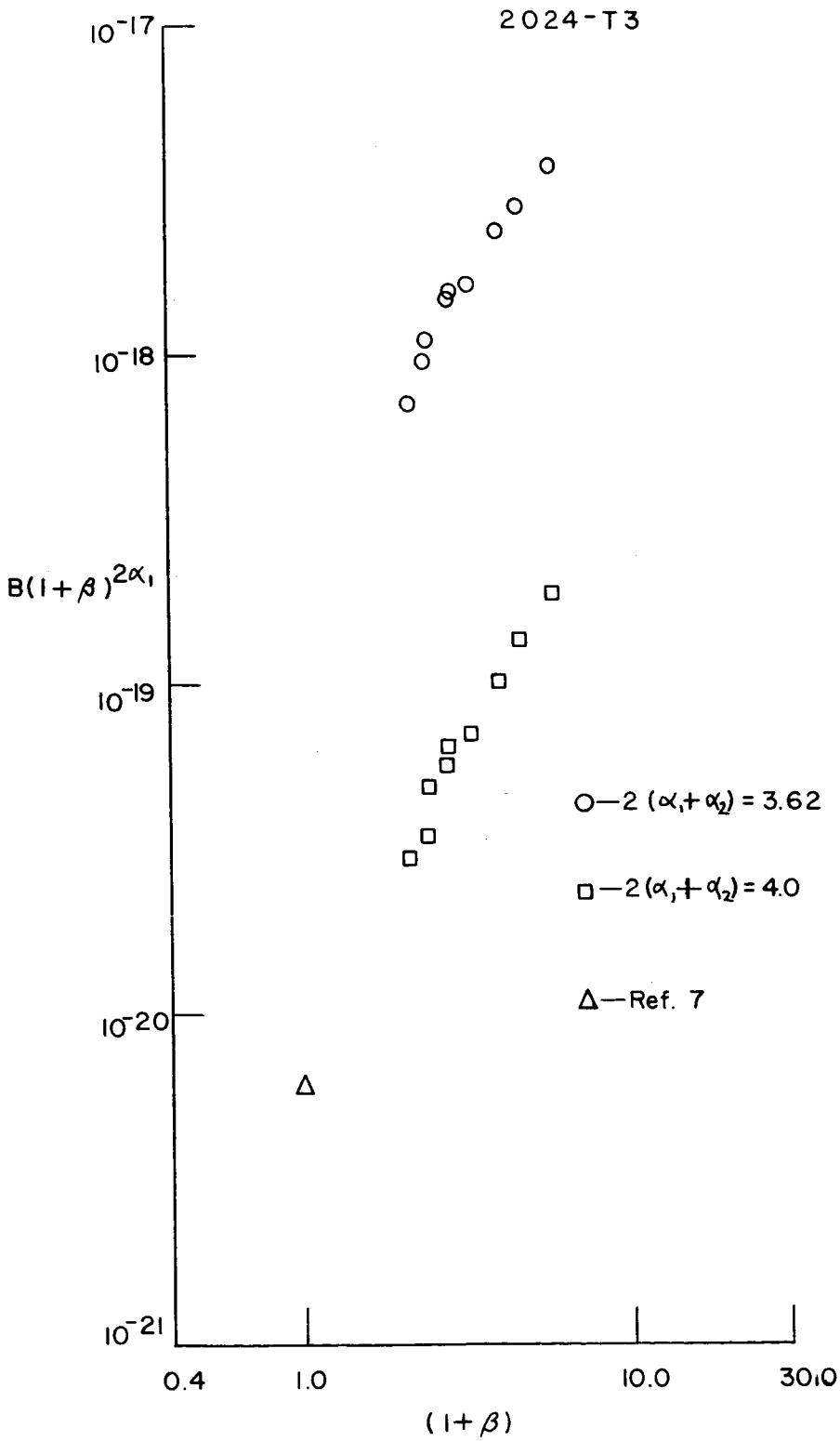
2024-T3
10^{-17}
10^{-18}
10^{-19}
10^{-20}
10^{-21}
$B(1+\beta)^{2\alpha_1}$
○—2 $(\alpha_1+\alpha_2)$ = 3.62
□—2 $(\alpha_1+\alpha_2)$ = 4.0
Δ—Ref. 7
0.4
1.0
10.0
30.0
$(1+\beta)$

FIGURE 8.

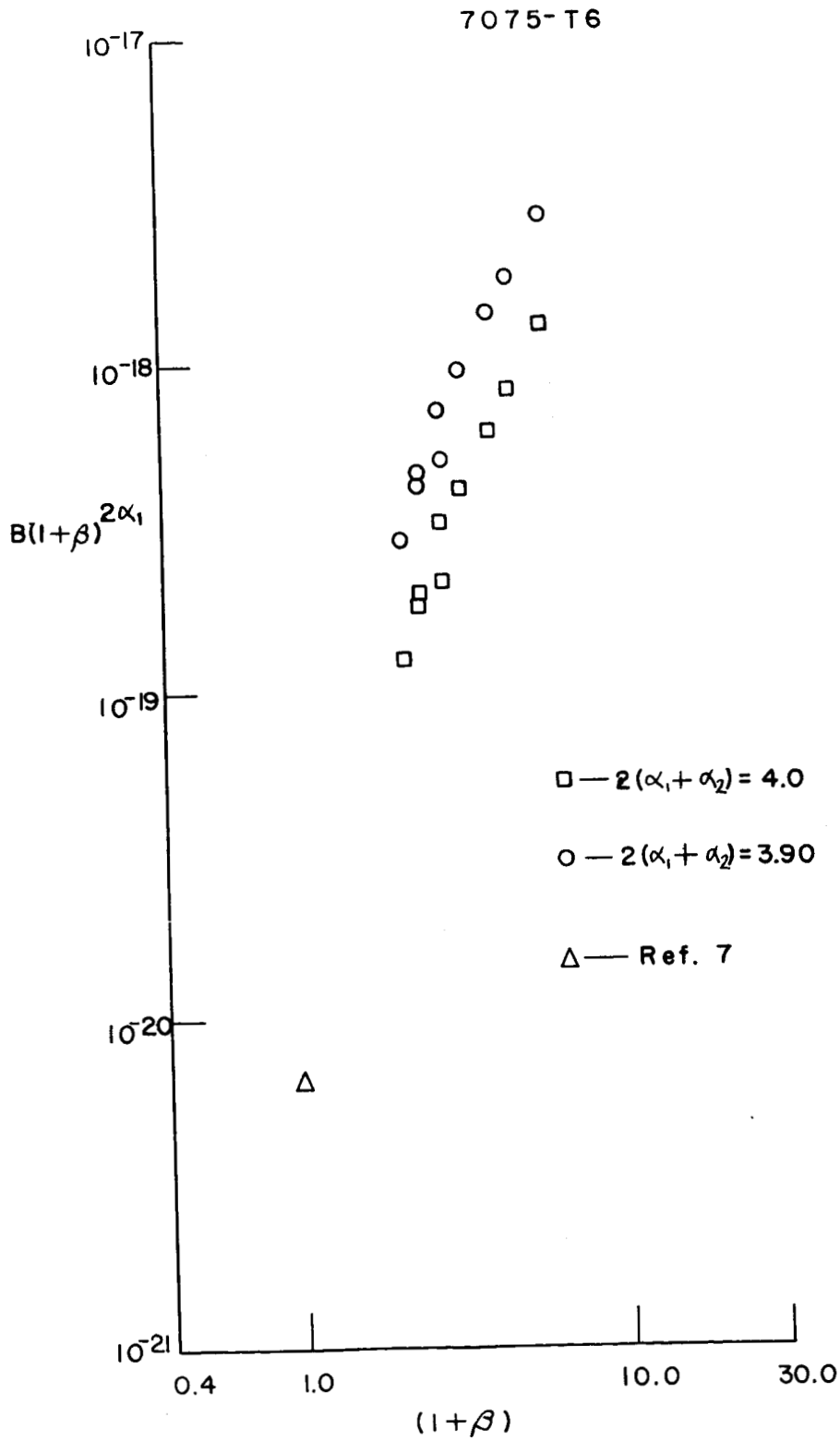
7075-T6
10^{-17}
10^{-18}
10^{-19}
10^{-20}
10^{-21}
$B(1+\beta)^{2\alpha_1}$
□ — $2(\alpha_1+\alpha_2) = 4.0$
○ — $2(\alpha_1+\alpha_2) = 3.90$
△ — Ref. 7
0.4
1.0
10.0
30.0
$(1+\beta)$